CrystEngComm

A perspective on underlying crystal growth mechanisms in biomineralization: solution mediated growth versus nanosphere particle accretion

SCHOLARONE™
Manuscripts

A perspective on underlying crystal growth mechanisms in biomineralization: solution mediated growth versus nanosphere particle accretion

Assaf Gal, Steve Weiner, and Lia Addadi

Department of Structural Biology, Weizmann Institute of Science, Rehovot, Israel 76100

Abstract

Many organisms form crystals from transient amorphous precursor phases. In the cases where the precursor phases were imaged, they consist of nanosphere particles. Interestingly, some mature biogenic crystals also have nanosphere particle morphology, but some are characterized by crystallographic faces that are smooth at the nanometer level. There are also biogenic crystals that have both crystallographic faces and nanosphere particle morphology. This highlight presents a working hypothesis, stating that some biomineralization processes involve growth by nanosphere particle accretion, where amorphous nanoparticles are incorporated as such into growing crystals and preserve their morphology upon crystallization. This process produces biogenic crystals with a nanosphere particle morphology. Other biomineralization processes proceed by ion-by-ion growth, and some cases of biological crystal growth involve both processes. We also identify several biomineralization processes which do not seem to fit this working hypothesis. It is our hope that this highlight will inspire studies that will shed more light on the underlying crystallization mechanisms in biology.

1. Introduction

Using a thermodynamic approach, nucleation theory well explains crystal nucleation and growth from supersaturated solutions, in ionic or molecular crystals.[1, 2] The theory describes the nucleating system as a homogeneous phase where fluctuations occur, creating metastable aggregates of solute molecules or ions. Some of these aggregates reach a critical size, beyond which further addition of ions is favored over dissolution, such that they continue to grow and eventually lead to the formation of precipitates. This growth mechanism of ionic crystals occurs as a result of ion-by-ion attachment to the surfaces of the growing crystal. The crystal morphology reflects the growth kinetics of the crystal in different crystallographic orientations (Figure 1 A),[3, 4] and this is determined by the distribution of the ionic interactions within the crystal lattice. The stable crystal surfaces reflect the network of ionic interactions along the most stable crystal layers, and are thus smooth almost to the atomic level (Figure 1 B).

Biologically formed crystals usually do not have the expected characteristics of such solution grown crystals.[5, 6] Biogenic crystals are often characterized by unusual shapes, some of which are amazingly convoluted, and bear no relation to the crystal symmetry and display no stable crystal faces (Figure 1 C). Furthermore, it has been observed that mature crystalline biogenic minerals often have a texture composed of nanosphere particles (Figure 1 D), as was first observed by Dauphin in cephalopod shells.[7] Subsequent high resolution AFM and SEM studies showed that not only mature mollusk shells,[7] but also coral skeletons,[8] echinoderm skeletons,[9] sponge spicules,[10] brachiopod shells,[11, 12] and crustacean cuticles,[13] also have this most unusual nanoscale morphology for a mature crystal, namely that they are composed of nanosphere particles (Figure 2). The reasons for these unique characteristics must be related to the differences between biological crystallization pathways and solution-mediated crystal growth.
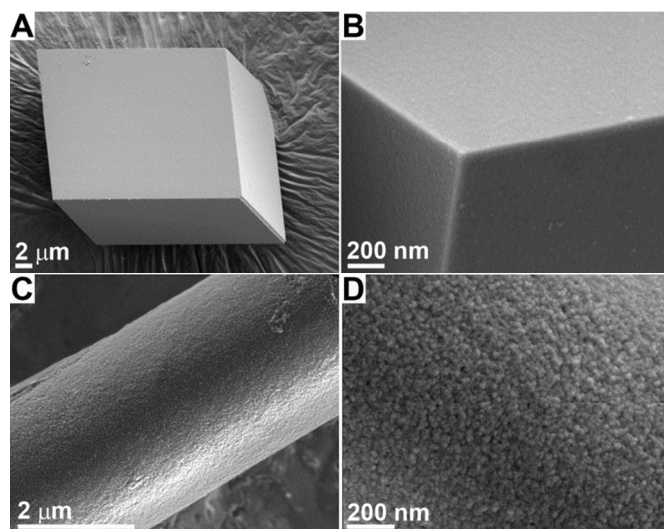
Figure 1: A) SEM images of a solution-grown calcite crystal showing the most stable rhombohedral faces; B) The faces are featureless down to the detection limit of the microscope. In contrast, the larval spicule of the sea urchin *Paracentrotus lividus*, is a single crystal of calcite that has a cylindrical shape (C); and has a surface morphology composed of aggregated nanosphere particles (D).
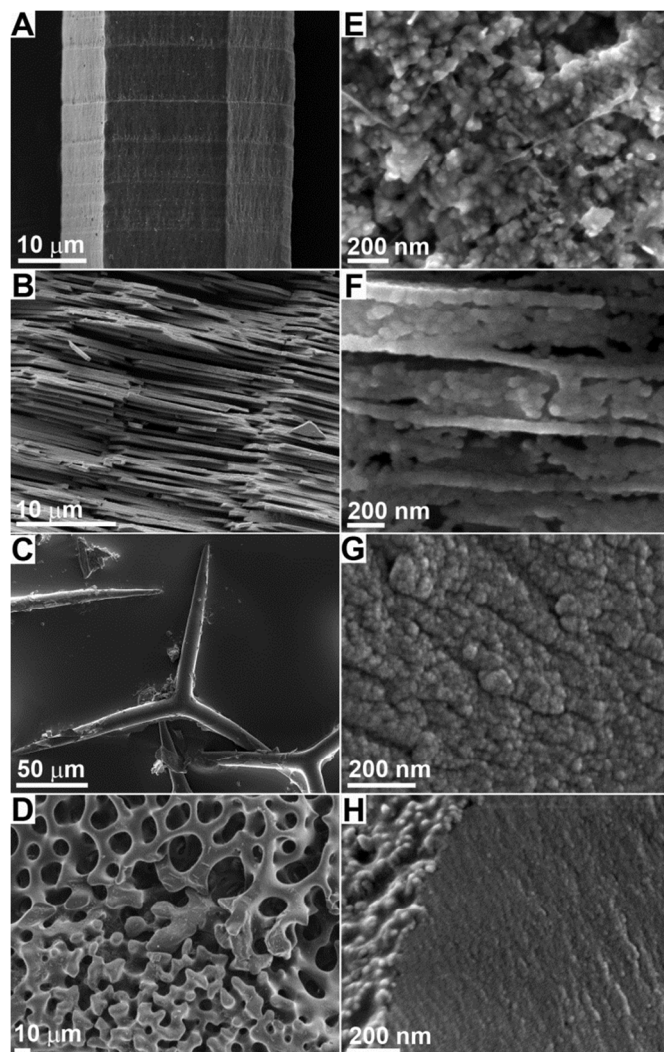

Figure 2: SEM images of biogenic crystalline elements (A-D), and high magnification images showing their nanosphere morphology (E-H).; A, E) An isolated calcitic prism of the bivalve *Atrina rigida*; B, F) Fracture in the nacreous layer of the shell of the cephalopod *Nautilus pompilius* showing the aragonitic tablets; C, G) Asymmetric triradiate spicule from the calcareous sponge *Sycon sp.*; D, H) Skeletal part from the brittle star *Ophiocoma wendtii*. Note that in E, F the surface was etched, such that the nanosphere particles are more prominent than in the untreated fracture surfaces of G, H.

In living organisms the cellular environment controls many of the properties of the crystallization pathway.[14] The first mineral formed is often within vesicles inside cells. In the few cases where this intracellular mineral has been characterized, it was found to be a highly disordered phase such as ferrihydrite,[15, 16] amorphous calcium carbonate,[17] and amorphous calcium phosphate or possibly polyphosphate.[18, 19] This initial disordered phase is subsequently transformed into a crystalline phase. The transformation may occur in a preformed extracellular matrix, as was first documented by Towe and Lowenstam in the case of the chiton tooth (Figure 3).[20] Thirty years after this initial discovery, Beniash et al. showed that the calcite single crystal of the sea urchin larval spicule also forms from an amorphous calcium carbonate (ACC) precursor phase.[17] In this case the transformation occurs within a membrane bound syncytium, with no evidence for the presence of associated liquid bulk water.[21] Within a relatively short time it was demonstrated that calcite forms from ACC in adult echinoderms,[22] crustaceans,[23] and annelids,[24, 25] aragonite from ACC in larval mollusk shells,[26, 27] anhydrous guanine crystals in fish skin from amorphous guanine,[28] and carbonated hydroxyapatite from ACP in tooth enamel[29] and in vertebrate bone.[18, 30] It is conceivable that the smooth and convoluted morphologies of the mature crystalline biogenic phases are due to the initial isotropic disordered phases adopting the shape of the pre-formed space into which they are deposited.
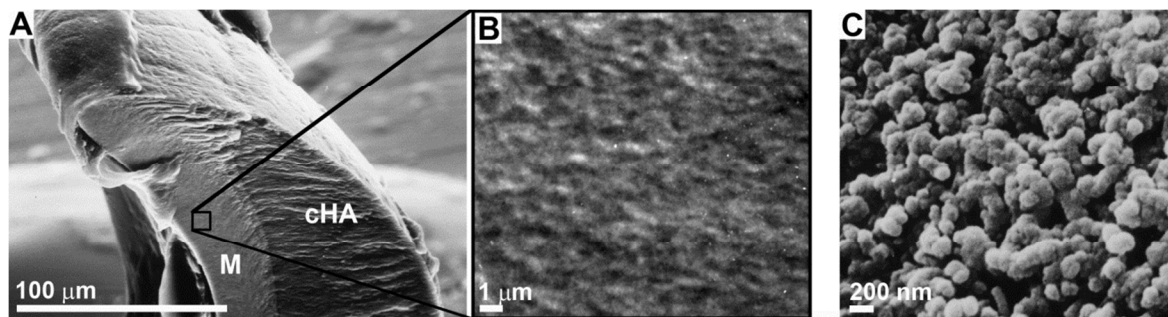
Figure 3: A, B) Cross section of a mature tooth from the chiton *Acanthopleura haddoni* showing the outer part mineralized with carbonated hydroxyapatite (cHA in the image) and the inner part mineralized with magnetite (M in the image); B) Magnification of the magnetite showing the nanosphere morphology; C) Nanosphere morphology of the ACP precursor to the carbonated hydroxyapatite of a maturing tooth.

When observed at high-magnification, biogenic amorphous minerals are composed of nanosphere particles with a typical size range of few tens of nanometers (Figure 3 C, Figure 4 A-C, E-G).[31, 32] This texture is present in amorphous phases that are stable during the lifetime of the organism, and in those that transform into a crystalline phase. This nanosphere particle morphology is also common in many amorphous phases produced *in vitro* (Figure 4 D, H).[33-37] This in turn raises the as yet unanswered question of whether or not the mature crystalline biogenic phases that also have this nanosphere particle texture, were inevitably formed from a transient amorphous precursor phase? Unfortunately very few cases have been studied *in vivo* where the transformation from the amorphous precursor phase to the crystalline mature phase, has been documented.
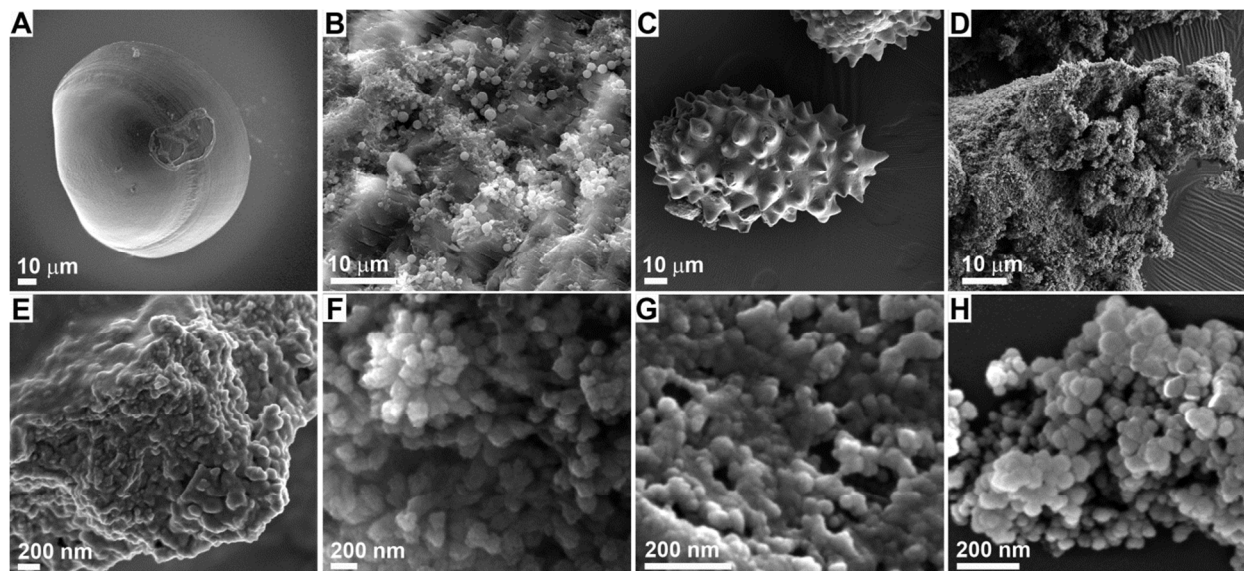
Figure 4: Some examples of biogenic and synthetic ACC phases. SEM images of bulk amorphous mineral phases (A-D), and high magnification images showing the common nanosphere morphology (E-H). A, E) Larval mollusk shell from *Mercenaria mercenaria*: the ACC particles are a precursor phase to aragonite; B, F) A fracture surface in the cuticle of the crab *Carcinus aestuarii* just after a molt cycle. The ACC particles are a precursor phase for calcite; C, G) A plant cystolith extracted from the leaf of *Ficus microcarpa*. The cystolith is composed of ACC particles that are stabilized *in vivo* and do not transform into a crystalline material; D, H) Synthetic ACC particles precipitated from a highly supersaturated solution. These amorphous phases, although composed of different materials formed under different conditions, and may be precursors for crystals or remain amorphous, all consist of nanosphere particles.

One of the best studied cases of precursor phase transformation is the spicule of the sea urchin embryo where nanosphere particles of ACC, initially formed inside intracellular vesicles, are deposited on the surface of the growing spicule and subsequently undergo crystallization at the site of deposition.[38, 39] The mechanism of transformation is thought to be a solid state transformation that propagates through the amorphous phase in three dimensions by secondary nucleation starting from the surface of the initially formed crystal.[40] Interestingly, the first mineral to form in the sea urchin embryo spicule is a perfect micron-sized rhombohedron (Figure 5 A).[41] A rhombohedron is the characteristic shape of a calcite crystal.

In the next step the initial rhombohedral crystal grows along the *a*-axes of the calcite lattice to form the tri-radiate spicule that does not express any crystal faces (Figure 5 A).[42, 43] A high magnification image of the rhombohedron surface shows the nanosphere particle morphology characteristic of ACC (Figure 5 B). A solid-state transformation of ACC to calcite cannot explain the rhombohedral habit that arises from the stability of the {104} lattice planes of calcite. Nevertheless, an ion-by-ion crystal growth mechanism cannot account for the nanosphere particle morphology of the spicule calcite rhombohedron. Resolving this paradox is essential in order to obtain a more complete mechanistic understanding of the transformation process in biomineralization. In this highlight we will present a conceptual framework that in our opinion may clarify aspects of this paradox. This conceptual framework is based on a series of *in vitro* studies of ACC transforming into calcite that we carried out.[44, 45] As will be shown, biogenic minerals are so diverse in their formation mechanisms that a single scheme can hardly reflect the natural complexity. However, we hope that the proposed viewpoint will inspire others to document the amorphous to crystalline transition *in vivo*, and in this way elucidate the mechanisms of this transformation.
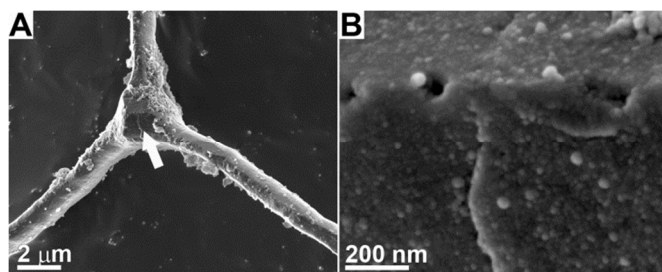

Figure 5: A) SEM images showing the initial calcite rhombohedron (arrow) of a *P. lividus* spicule and the three arms growing along its a-axes; B) High magnification of the rhombohedron surfaces showing the nanosphere particle morphology.

2. Crystal growth via nanosphere particle accretion

In the last decade many *in vitro* studies have been carried out on the factors that influence the transformation of disordered phases such as ACC and ACP into crystalline phases.[36, 46-50] Many of these studies start with highly saturated phases that then form precipitates,[51, 52] essentially following Ostwald's Rule of Stages. The initial mineral phases themselves may have unusual liquid-like properties,[53] or be more solid. The crystalline products reflect the different formation conditions, and are also greatly influenced by the size and surface properties of the confining volumes.[54]

In our *in vitro* experiments, we initially used a solid biogenic ACC phase (plant cystoliths) that transforms *in vitro* (not *in vivo*) readily into calcite,[44] surprisingly producing calcite crystals with a macroscopic rhombohedral morphology, but composed of spheres at the nanometer level. To understand the phenomenon in depth, we subsequently simplified the system using a synthetically generated kinetically stabilized ACC solid phase.[45] We suggest that crystal growth can proceed via two competing mechanisms. One mechanism involves the dissolution of ACC in an aqueous solution followed by crystal nucleation and ion-by-ion crystal growth. This is essentially the "classic" crystal growth mechanism, with the source of ions being the dissolving ACC phase, and the resultant crystal is in the form of the rhombohedron typical of calcite. In the second mechanism the ACC particles are partially stabilized by the presence of additives, either in the solution or in the bulk ACC phase. These additives stabilize the nanospheres sufficiently, such that they can migrate to the surface of the growing crystal, where they crystallize. The size of the perfect crystalline domains within the final crystal is several times larger than the initial particle, supporting the notion of crystal growth by propagation of nucleation from the initial crystal to the amorphous nanospheres. The additives that were tested are gel-forming molecules now known to be present in several different mineralized tissues,[44, 55-58], phosphate ions (common

in certain calcitic mineralized tissues, such as the crustacean cuticle),[59, 60] and biogenic macromolecules that were extracted from sea urchin spicules. The crystals that grew in the presence of these additives, also expressed the characteristic {104} stable faces of calcite, and were composed of nanosphere particles similar to the biogenic materials. The dual characteristics of these synthetic crystals raised the possibility that their growth involved two different processes acting simultaneously: ion-by-ion growth from solution and nanosphere ACC particle accretion followed by crystallization after contact with the crystalline substrate (Figure 6).

Observing biogenic minerals in light of the insights derived from the above experiments *in vitro*, we identify one extreme where crystal growth appears to proceed only via an ion-by-ion addition process, inferred from the presence of smooth crystallographic faces. The term "smooth" is in relation to the resolution of the SEM, namely less than about 2nm. The other extreme, where crystal growth proceeds via the accretion of nanosphere particles, is inferred from the presence of nanosphere particle morphology. The spherical particles typically observed in biominerals are around 20nm or larger. There are however biogenic crystal growth processes that appear to involve both mechanisms, and those that seem to not fit into any well-defined category. Below we briefly describe several cases of biogenic crystal formation that appear to involve only the extreme mechanisms, some that appear to involve both mechanisms, and two that do not seem to fit the scheme at all.
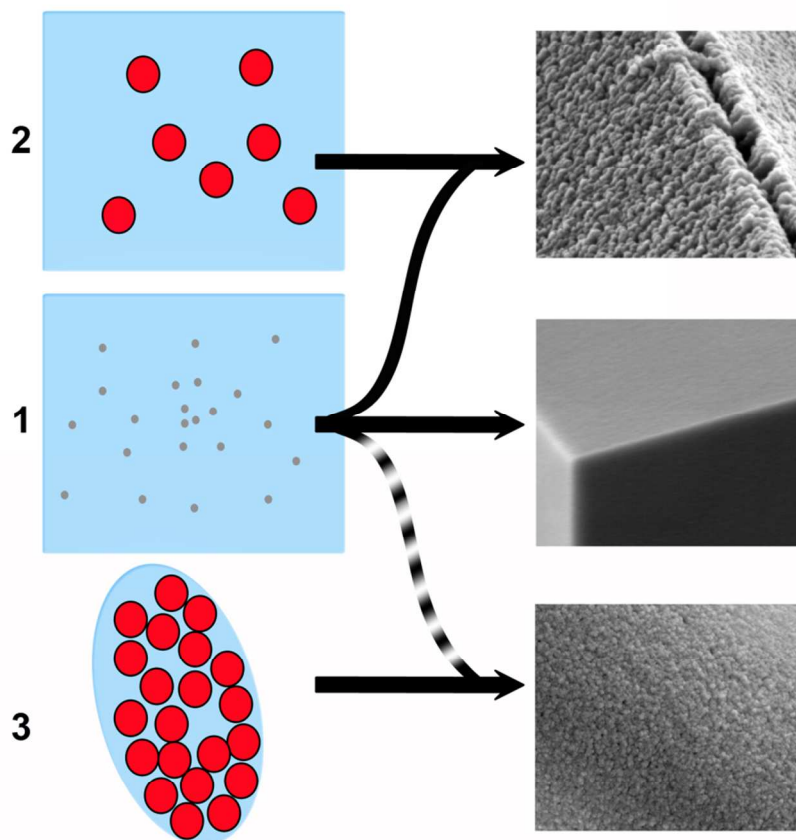
Figure 6: Schematic representation of the different processes that might be involved in crystal growth: 1) Crystals can grow from ions in solution resulting in faceted crystals with smooth surfaces; 2) In the presence of additives, amorphous nanosphere particles can migrate to the surface of a growing crystal where they crystallize. Under such conditions ion-by-ion growth occurs concomitantly, and the resulting crystals will have crystallographic faces with nano-particulate morphology; 3) shows the pathway that is proposed to be dominant in many biological systems, where the nanosphere particles are deposited into a confined space that molds the crystal shape. The role of ions in this process is not completely clear.

3. Case Studies

Limpet teeth. Limpets (marine mollusks) form mineralized teeth on their radula, a tongue-like organ that consists of continuously forming rows of teeth. The first mineral to form in shallow water limpet teeth is goethite (α-FEOOH) and later silica is precipitated to fill in the spaces between the goethite crystals (Figure 7 A).[61] In the teeth of the limpet *Patella caerulea* no evidence was observed for an amorphous precursor phase during goethite formation,[62] even though the stages of formation can be conveniently tracked row by row (as was done for the chiton).[20, 63, 64] The goethite crystals are a few hundreds of nanometers in size and electron

microscopy clearly showed a crystal habit that is consistent with the goethite crystal structure (Figure 7 B).[62] There is no evidence of a nanosphere morphology inside or on the surfaces of these crystals. The crystals grow inside a preformed organic matrix composed primarily of the polysaccharide chitin. The crystals do not have a uniform orientation but are more or less aligned with the chitinous network. In addition, a few types of morphologies are observed showing different sets of crystallographic planes.[62] These properties of the limpet teeth goethite crystals are consistent with an ion-by-ion crystal growth process and show no evidence for the particle accretion process.
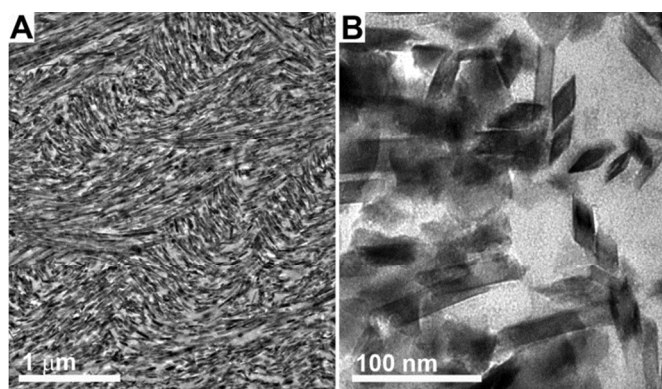

Figure 7: TEM micrographs of a transverse section from a tooth of the limpet *Patella caerulea*. A) The fully mineralized tooth is densely packed with goethite crystals along the chitin fibers. B) High magnification shows many cross sections of crystals with distinct crystallographic faces.

Plant raphides. Higher plants precipitate a large variety of calcium oxalate crystals with different morphologies, in various anatomical locations and composed of different polymorphs.[65, 66] The crystals form inside a vacuole located in a specialized cell that controls the crystal growth.[66] One distinct calcium oxalate crystal morphology found in plants is the needle-like crystals called raphides that are organized into bundles.[67] Each crystal is enveloped by an organic sheath.[68] Each crystal has prismatic faces capped by pointy ends that are also delimited by crystallographic planes (Figure 8). In some species raphide crystals are twinned.[69] The crystals are tens of micrometers long, but their widths are sometimes only 500 nm. Even the smallest crystals express crystallographic planes, and there is no indication that they possess a nanosphere particle texture.

Solution grown calcium oxalate monohydrate crystals usually have a simple tabular habit that reflects the lattice symmetry.[70] Other types of biogenic calcium oxalates have very different morphologies, ranging from simple bulky crystals to an aggregate of platelets.[66] The elongated prismatic habit of the biogenic raphide crystals with its extraordinary aspect ratio implies certain modifications of the crystallization process exerted by the cellular environment. Altogether the properties of calcium oxalate raphides are consistent with ion-mediated crystal growth that is affected by the cellular context in which they form.
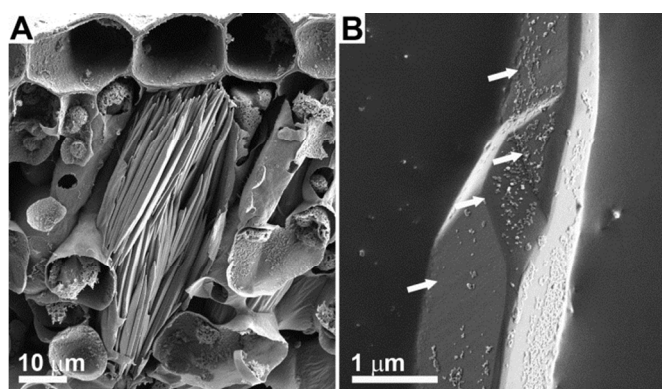

Figure 8: A) SEM image of a cross section in a critical-point-dried leaf of *Bougainvillea glabra*. A bundle of calcium oxalate raphide crystals is located inside the photosynthetic tissue. B) An image of the tip of isolated crystal that shows the smooth crystallographic faces (some faces are indicated by arrows). Some organic debris is adsorbed onto parts of the crystal surfaces.

Barnacle shell. Barnacles are a class of marine sessile crustaceans (Cirripedia) that build a calcitic shell.[71] A structural study of different shell elements shows that the mineral is composed of polycrystalline calcite crystals that are enveloped by a non-proteinaceous sulfate-rich polymer that behaves as a hydro-gel.[55, 72, 73] The crystals express the most stable crystallographic faces of calcite (Figure 9 A). When the crystals were examined at high-resolution using an SEM, a nanosphere texture was revealed (Figure 9 B). The barnacle shell crystals, with microscopic rhombohedral habit and nanoscale morphology, show characteristics of both the ion-mediated process and the particle accretion process.
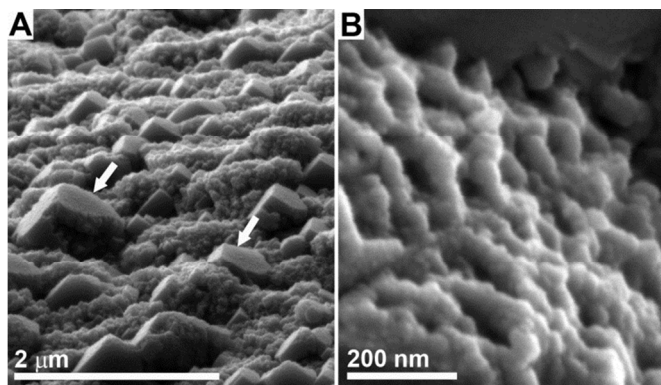
Figure 9: A) SEM image of the growing surface of the shell of the barnacle *Balanus amphitrite*. Rhombohedral calcite crystals emerge from the surface that is covered with organic matrix. B) High magnification image of the mineral showing the nanosphere particle morphology.

Fish otoliths. The aragonite crystals of fish otoliths grow inside a dense organic matrix with hydro-gel characteristics.[58, 74-76] Otoliths have a porous polycrystalline array composed of approximately aligned needle-shaped crystals (Figure 10 A). This crystal morphology is typical of inorganically formed aragonite crystals. When observed at high magnifications otolith aragonite crystals do show nanosphere particle morphology (Figure 10 B).[58, 77]
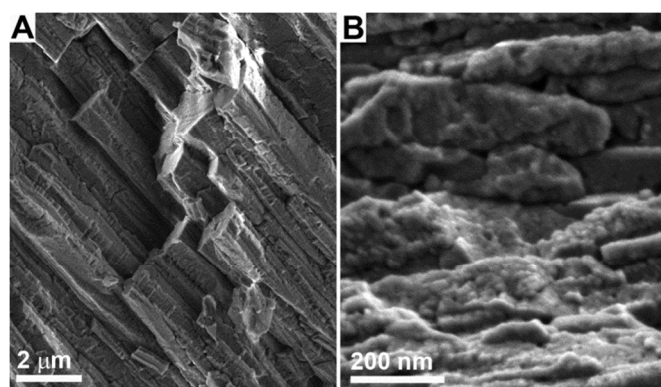

Figure 10: SEM images at low (A) and high (B) magnifications of a fracture surface of an otolith from the fish *Seriphus politus*. The needles of the aragonite crystals show crystal faces composed of nanosphere particles.

Crystals with convoluted morphologies and nanosphere particle textures. Many organisms form crystals that have convoluted morphologies that do not resemble crystal faces and also have nanosphere particle morphologies. Examples are the calcite single crystals of echinoderms (Figure 1 C, D, Figure 4 A, F),[78] calcitic sponge spicules (Figure 4 C, G),[10] the oriented crystal arrays of aragonite and calcite that make up the different shell structures of mollusks (Figure 4 A, B, E, F),[7] and the calcitic shells of brachiopods.[11, 12]

4. Working hypothesis

We propose that many crystal growth mechanisms in biology can involve solution mediated ion-by-ion growth, or particle accretion, or a combination of both processes. When both processes occur together, necessary conditions are the presence of small amounts of liquid water, possibly in part being derived from the initial ACC phase, and stabilization of the particles in this microenvironment.

Perspective on the mechanisms that control particle-accretion growth in biomineralization

How does transformation from a disordered to an ordered phase occur in the nanosphere particle accretion process? In the cases of ACC and ACP the amorphous phase is kinetically stable at ambient temperatures and does not undergo crystallization if it is kept dry.[79, 80] The presence of water in the microenvironment of the transformation is a driving force for the transformation.[81] The contribution of the water molecules is probably a key factor also in determining the balance between the ion-mediated and the particle-mediated processes. In environments such as in a gel, the activity of water is reduced relative to the bulk solution, because some of the water is associated with the gelator molecules.[56] The reduced water activity presumably slows down the disordered nanosphere dissolution such that the nanospheres can persist as a disordered phase during translocation to the surface of the growing crystal, where they crystallize upon contact with the ordered substrate. The aqueous environment obviously involves a certain amount of dissolution, but not sufficient to completely dissolve the nanospheres. Additives such as phosphate ions or certain macromolecules can also lower the dissolution rate of the amorphous nanospheres, presumably by binding to their surface.[82, 83] The two competing processes of ion-by-ion growth and growth by particle accretion, reach a balance

that reflects the kinetic competition between the processes. For a more detailed discussion, see Gal et al.[45]

The extreme case of the particle accretion process is observed in the sea urchin spicule,[40] and presumably by inference in adult echinoderm skeletal parts and in calcareous sponge spicules, all of which lack any expressed crystal habits. Even in these cases that seem to occur in the absence of bulk water,[21] water must play a role in facilitating the transformation. Proof of this being the case is that in the total absence of water the amorphous phase is stabilized. We can speculate that the first-formed rhombohedral shaped crystal that forms in the sea urchin larva may have been produced in an initial environment richer in water. This environment subsequently changes into a confined space where the amorphous nanospheres are in direct contact with the spicule envelope. The barnacle shell and the fish otolith crystals are possibly additional examples of the task of water in mediating the transformation of ACC into a crystalline phase inside a hydro-gel, and in determining the morphology of the mature mineral phase.

One additional observation made in the adult sea urchin spines, as well as in calcareous sponge spicules, which is difficult to reconcile with a pure particle accretion growth mechanism, is that macromolecules occluded inside the mature crystal tend to concentrate on certain crystal planes and not others.[84] If the macromolecules were initially present in the amorphous precursor phase, the only way in which they can align themselves on specific planes during the crystallization process, is through a process mediated by water. Such alignment must involve substantial molecular rearrangement. The alternative possibility that the macromolecules are independently introduced into the crystal growth environment at specific locations is difficult to envisage. It would therefore be interesting to determine how much water is present in the local environment of crystallization *in vivo*, and what are the locations and the dynamics of this water.

We do not know whether the initially deposited nanosphere particles *in vivo* are more solid-like or more liquid-like with an extremely high salt concentration; a difference that is extremely difficult to determine if the phase is highly disordered. Hypotheses that have been formulated regarding the precipitation of the amorphous phase include processes such as spinodal decomposition, liquid-liquid separation, or solid-liquid separation.[35, 85-87]

It will require much more effort to obtain experimental evidence to differentiate between these options *in vivo*, especially when bearing in mind that in many cases the initial mineral phase is produced in vesicles within cells.[14] In the mature biogenic products, there are cases where the ACC particles are clearly in a solid phase, such as the stable ACC containing mineralized tissues, and the forming sea urchin larval spicule, as these materials can be isolated and characterized as such. Two types of information are needed in order to relate fundamental chemical studies to biology: 1) to characterize the cellular processes that lead to the formation of the initial precursor phase. In this respect, it is important not to confuse the nanospheres discussed here (10-20 nm) with the one order of magnitude smaller pre-nucleation aggregates that are extensively discussed in relation to amorphous and crystalline phase formation *in vitro*.[51, 52] 2) The environment mediating the transformation of the particle from the initial phase separation to the crystallization: In theory, this environment may range from a bulk solution facilitating oriented attachment of crystallites,[88] to a confined volume that accommodates amorphous particle aggregation followed by secondary nucleation on the propagating crystal.[89]

5. Interesting exceptions.

Magnetotactic bacteria form a chain of magnetite crystals that play a role in the orientation of the bacteria relative to the earth's magnetic field.[90, 91] The crystals form inside vesicles that are aligned along a fibrous element, collectively termed the magnetosome.[92, 93] The magnetite crystals are a few tens of nanometers in size and their crystal morphology is species-specific.[91]

Many species produce magnetite crystals with well-defined crystal habits, whereas other species produce crystals with a smooth and rounded shape.[91] The magnetite crystals do form via an amorphous iron-phosphate precursor phase,[94] but high resolution images show no evidence of a nanosphere particle texture in the mature crystals. Furthermore, the chemical composition of the precursor phase differs from that of the mature crystalline phase.[94] All these characteristics do not fit into our simplified scheme.

Bone crystals are perhaps the smallest crystals known to be formed in biology (Figure 11). The crystals are plate-shaped,[95, 96] and their thicknesses range between 2 and 4 nm,[97] which is almost an order of magnitude smaller than the usual diameters of the nanospheres that make up amorphous phases of calcium carbonate or calcium phosphate. Yet, the crystals do form *in vivo* via a disordered phase with characteristics of an ACP,[18] and/or octacalcium phosphate (OCP)-like precursor phase,[98] with nanospheres of 10-20nm in diameter. Many of the crystals form inside the collagen fibril,[6] and it is difficult to conceive how 10-20nm diameter solid particles penetrate into the fibril. A liquid-like nature of the precursor phase may be a plausible explanation for the mineral infiltration of the fibrils.[99] The OCP-like intermediate phase may well be the reason why these carbonated hydroxyapatite crystals with their hexagonal atomic symmetry have a shape that more closely reflects the triclinic symmetry of OCP. Note too that nanosphere particles have been observed in mature bone together with the abundant plate-shaped crystals.[100] Bone crystal growth clearly does not fit into our scheme either.
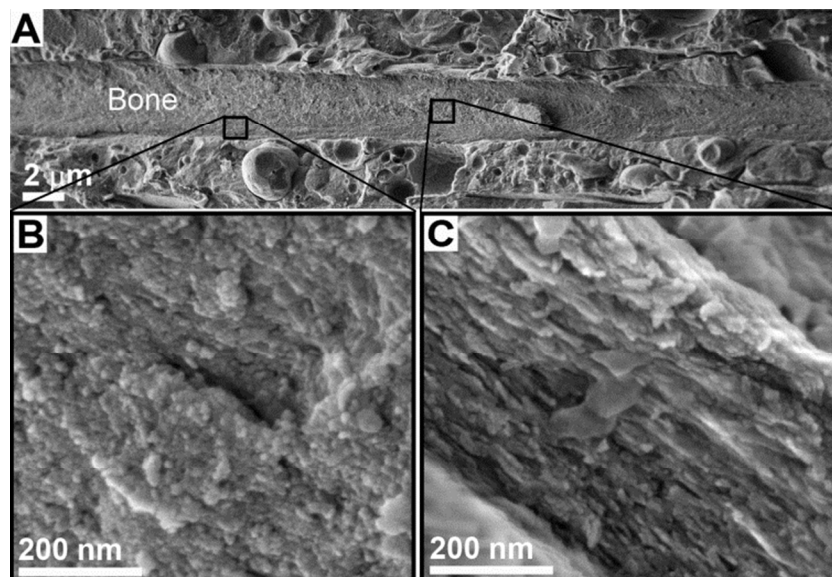
Figure 11: Cryo-SEM images taken from a high-pressure frozen and freeze-fractured fin of a mature zebrafish (*Danio rerio*). A) Low magnification image showing the continuously growing fin bone surrounded by the cellular tissue; B) High magnification image of an area close to the bone surface filled with newly deposited nanosphere particles; C) High magnification image of an area in the interior of the bone showing the carbonated hydroxyapatite crystals with thickness lower than the diameter of the initial particles and no nanosphere morphology.

6. Conclusions

Many, but not all, mineral formation processes in biology involve the initial formation of an amorphous precursor phase with its characteristic nanosphere particle morphology. This same morphology is preserved in the mature biogenic crystals of some, but not all biomineralization products. Based on the presence of expressed crystal faces that indicate growth by ions, or the presence of the nanosphere morphology in mature crystals that indicate growth by particle accretion, we classify different biomineralization processes. We identify two extreme crystal growth processes: ion-by-ion growth and growth by particle accretion. We also find that some crystals form by a combination of these two end member processes, and some do not appear to fit directly into this scheme. This somewhat simplistic view of crystal growth in biology may help to clarify the different underlying mechanisms that are involved in different biomineralization processes, and inspire new experiments aim at elucidating the specific crystallization pathways that occur *in vivo*.

Acknowledgments

References

1. J. W. Gibbs, *Transactions of the Connecticut Academy of Arts and Sciences*, 1876, **2**, 108-248; 343-524.
2. J. J. De Yoreo and P. G. Vekilov, *Rev. Mineral. Geochem.*, 2003, **54**, 57-93.
3. P. Hartman and W. G. Perdok, *Acta Crystallogr.*, 1955, **8**, 49-52.
4. I. Weissbuch, L. Addadi and L. Leiserowitz, *Science*, 1991, **253**, 637-645.
5. K. Simkiss and K. Wilbur, *Biomineralization. Cell Biology and Mineral Deposition.*, Academic Press, Inc., San Diego, 1989.
6. H. A. Lowenstam and S. Weiner, *On Biomineralization*, Oxford University Press, New York, 1989.
7. Y. Dauphin, *Palaontologische Zeitschrift*, 2001, **75**, 113-122.
8. A. Meibom, J. P. Cuif, F. O. Hillion, B. R. Constantz, A. Juillet-Leclerc, Y. Dauphin, T. Watanabe and R. B. Dunbar, *Geophys. Res. Lett.*, 2004, **31**.
9. J. Seto, Y. R. Ma, S. A. Davis, F. Meldrum, A. Gourrier, Y. Y. Kim, U. Schilde, M. Sztucki, M. Burghammer, S. Maltsev, C. Jager and H. Colfen, *Proc. Natl. Acad. Sci.*, 2012, **109**, 7126-7126.
10. I. Sethmann, R. Hinrichs, G. Worheide and A. Putnis, *J. Inorg. Biochem.*, 2006, **100**, 88-96.
11. M. Cusack, Y. Dauphin, P. Chung, A. Perez-Huerta and J. P. Cuif, *J. Struct. Biol.*, 2008, **164**, 96-100.
12. E. Griesshaber, K. Kelm, A. Sehrbrock, W. Mader, J. Mutterlose, U. Brand and W. W. Schmahl, *Eur. J. Mineral.*, 2009, **21**, 715-723.
13. A. Al-Sawalmih, C. Li, S. Siegel, H. Fabritius, S. Yi, D. Raabe, P. Fratzl and O. Paris, *Adv. Funct. Mater.*, 2008, **18**, 3307-3314.
14. S. Weiner and L. Addadi, *Annu. Rev. Mater. Res.*, 2011, **41**, 21-40.
15. M. H. Nesson and H. A. Lowenstam, in *Magnetite Biomineralization and Magnetoreception in Organisms*, Springer, 1985, pp. 333-363.
16. R. Cruz and M. Farina, *Mar. Biol.*, 2005, **147**, 163-168.
17. E. Beniash, J. Aizenberg, L. Addadi and S. Weiner, *Proc. R. Soc. London B Ser.*, 1997, **264**, 461-465.

18. J. Mahamid, A. Sharir, L. Addadi and S. Weiner, *Proc. Natl. Acad. Sci. U.S.A.*, 2008, **105**, 12748-12753.
19. S. Boonrungsiman, E. Gentleman, R. Carzaniga, N. D. Evans, D. W. McComb, A. E. Porter and M. M. Stevens, *Proc. Natl. Acad. Sci. U.S.A.*, 2012, **109**, 14170-14175.
20. K. M. Towe and H. A. Lowenstam, *J. Ultrastructure Res.*, 1967, **17**, 1-13.
21. E. Beniash, L. Addadi and S. Weiner, *J. Struct. Biol.*, 1999, **125**, 50-62.
22. Y. Politi, T. Arad, E. Klein, S. Weiner and L. Addadi, *Science*, 2004, **306**, 1161-1164.
23. R. Dillaman, S. Hequembourg and M. Gay, *J. Morphol.*, 2005, **263**, 356-374.
24. L. Gago-Duport, M. J. I. Briones, J. B. Rodriguez and B. Covelo, *J. Struct. Biol.*, 2008, **162**, 422-435.
25. M. R. Lee, M. E. Hodson and G. N. Langworthy, *Min. Mag.*, 2008, **72**, 257-261.
26. I. M. Weiss, N. Tuross, L. Addadi and S. Weiner, *J. Exp. Zool.*, 2002, **293**, 478-491.
27. B. Hasse, H. Ehrenberg, J. Marxen, W. Becker and M. Epple, *Chem. Eur. J.*, 2000, **6**, 3679-3685.
28. D. Gur, Y. Politi, B. Sivan, P. Fratzl, S. Weiner and L. Addadi, *Angew. Chem. Int. Ed.*, 2013, **125**, 406-409.
29. E. Beniash, R. A. Metzler, R. S. K. Lam and P. U. P. A. Gilbert, *J. Struct. Biol.*, 2009, **166**, 133-143.
30. J. Mahamid, A. Sharir, D. Gur, E. Zelzer, L. Addadi and S. Weiner, *J. Struct. Biol.*, 2011, **174**, 527-535.
31. H. A. Lowenstam and G. R. Rossman, *Chem. Geol.*, 1975, **15**, 15-51.
32. H. Lowenstam and S. Weiner, *Science*, 1985, **227**, 51-53.
33. J. Rieger, T. Frechen, G. Cox, W. Heckmann, C. Schmidt and J. Thieme, *Faraday Discuss.*, 2007, **136**, 265-277.
34. A. Sugawara, T. Ishii and T. Kato, *Angew. Chem. Int. Ed.*, 2003, **42**, 5299-5303.
35. M. Faatz, F. Gröhn and G. Wegner, *Adv. Mater.*, 2004, **16**, 996-1000.
36. L. B. Gower, *Chem. Rev.*, 2008, **108**, 4551-4627.
37. R. K. Iler, *The chemistry of silica: solubility, polymerization, colloid and surface properties, and biochemistry*, Wiley, New York 1979.
38. N. Vidavsky, S. Addadi, J. Mahamid, E. Shimoni, D. Ben-Ezra, M. Shpigel, S. Weiner and L. Addadi, *Proc. Natl. Acad. Sci. U.S.A.*, 2014, **111**, 39-44.
39. Y. U. T. Gong, C. E. Killian, I. C. Olson, N. P. Appathurai, A. L. Amasino, M. C. Martin, L. J. Holt, F. H. Wilt and P. U. P. A. Gilbert, *Proc. Natl. Acad. Sci. U.S.A.*, 2012, **109**, 6088-6093.
40. Y. Politi, R. A. Metzler, M. Abrecht, B. Gilbert, F. H. Wilt, I. Sagi, L. Addadi, S. Weiner and P. Gilbert, *Proc. Natl. Acad. Sci. U.S.A.*, 2008, **105**, 17362-17366.
41. K. Okazaki and S. Inoue, *Dev. Growth Differ.*, 1976, **18**, 413-434.
42. F. H. Wilt, *Dev. Biol.*, 2005, **280**, 15-25.
43. K. Okazaki, K. McDonald and S. Inoue, in *The mechanisms of biomineralization in animals and plants*, ed. Omori M. and Watabe N., Tokai University Press, Tokyo, 1980, 159-168.
44. A. Gal, W. Habraken, D. Gur, P. Fratzl, S. Weiner and L. Addadi, *Angew. Chem. Int. Ed.*, 2013, **52**, 4867-4870.
45. A. Gal, K. Kahil, N. Vidavsky, R. T. DeVol, P. U. Gilbert, P. Fratzl, S. Weiner and L. Addadi, *Adv. Funct. Mater.*, 2014, **24**, 5420-5426.
46. F. C. Meldrum and H. Cölfen, *Chem. Rev.*, 2008, **108**, 4332-4432.
47. F. Nudelman and N. A. J. M. Sommerdijk, *Angew. Chem. Int. Ed.*, 2012, **51**, 6582-6596.
48. Q. Hu, M. H. Nielsen, C. L. Freeman, L. M. Hamm, J. Tao, J. R. I. Lee, T. Y. J. Han, U. Becker, J. H. Harding, P. M. Dove and J. J. De Yoreo, *Faraday Discuss.*, 2012, **159**, 509-523.
49. F. M. Michel, J. MacDonald, J. Feng, B. L. Phillips, L. Ehm, C. Tarabrella, J. B. Parise and R. J. Reeder, *Chem. Mater.*, 2008, **20**, 4720-4728.
50. J. Aizenberg, D. A. Muller, J. L. Grazul and D. R. Hamann, *Science*, 2003, **299**, 1205-1208.
51. D. Gebauer, A. Volkel and H. Colfen, *Science*, 2008, **322**, 1819-1822.

52.   E. M. Pouget, P. H. H. Bomans, J. A. C. M. Goos, P. M. Frederik, G. de With and N. A. J. M. Sommerdijk, *Science*, 2009, **323**, 1455-1458.
53.   L. B. Gower and D. J. Odom, *J. Cryst. Growth*, 2000, **210**, 719-734.
54.   C. J. Stephens, S. F. Ladden, F. C. Meldrum and H. K. Christenson, *Adv. Funct. Mater.*, 2010, **20**, 2108-2115.
55.   G. M. Khalifa, S. Weiner and L. Addadi, *Cryst. Growth Des.*, 2011, **11**, 5122-5130.
56.   E. Asenath-Smith, H. Y. Li, E. C. Keene, Z. W. Seh and L. A. Estroff, *Adv. Funct. Mater.*, 2012, **22,** 2891-2914.
57.   F. Nudelman, B. A. Gotliv, L. Addadi and S. Weiner, *J. Struct. Biol.*, 2006, **153**, 176-187.
58.   U. Lins, M. Farina, M. Kurc, G. Riordan, R. Thalmann, I. Thalmann and B. Kachar, *J. Struct. Biol.*, 2000, **131**, 67-78.
59.   A. P. Vinogradov, *The Elementary Chemical Composition of Marine Organisms*, Sears Foundation for Marine Research II. Yale University, New Haven, 1953.
60.   A. Al-Sawalmih, C. H. Li, S. Siegel, P. Fratzl and O. Paris, *Adv. Mater.*, 2009, **21**, 4011-4015.
61.   H. A. Lowenstam, *Science*, 1971, **171**, 487-490.
62.   E. D. Sone, S. Weiner and L. Addadi, *Cryst. Growth Des.*, 2005, **5**, 2131-2138.
63.   K. M. Towe, *Science*, 1967, 157, 1048-&.
64.   J. L. Kirschvink and H. A. Lowenstam, *Earth Planet Sc. Lett.*, 1979, **44**, 193-204.
65.   T. Pobeguin, *Etude physico-chimique. Ann. Sci. nat., Bot*, 1943, **4**, 1-93.
66.   V. R. Franceschi and P. A. Nakata, *Ann. Rev. Plant Bio,*, 2005, **56**, 41-71.
67.   H. J. Arnott and F. G. E. Pautard, in *Biological calcification: cellular and molecular aspects*, ed. H. Schraer, Appelton Century Crofts, New York, 1970, pp. 375-446.
68.   M. A. Webb, J. M. Cavaletto, N. C. Carpita, L. E. Lopez and H. J. Arnott, *Plant J.*, 1995, **7**, 633-648.
69.   H. J. Arnott and M. A. Webb, *Int. J. Plant Sci.*, 2000, **161**, 133-142.
70.   A. Frey-Wyssling, *Am. J. Bot.*, 1981, **68**, 130-141.
71.   W. Meigen, *Ber. Naturf. Ges. Freiburg I.B.*, 1903, **13**, 1-55.
72.   W. Klepal and H. Barnes, *J. Exp. Mar. Biol. Ecol.*, 1975, **17**, 269-296.
73.   A. B. Rodríguez-Navarro, C. CabraldeMelo, N. Batista, N. Morimoto, P. Alvarez-Lloret, M. Ortega-Huertas, V. M. Fuenzalida, J. I. Arias, J. P. Wiff and J. L. Arias, *J. Struct. Biol.*, 2006, **156**, 355-362.
74.   E. T. Degens, W. G. Deuser and R. L. Haedrich, *Mar. Biol.*, 1969, 2, 105-113.
75.   R. W. Gauldie and D. G. A. Nelson, *Comp. Biochem. Physiol., A: Physiol.*, 1988, **90**, 501-509.
76.   G. Falini, S. Fermani, S. Vanzo, M. Miletic and G. Zaffino, *Eur. J. Inorg. Chem.*, 2005, 162-167.
77.   Y. Dauphin and E. Dufour, *Micron*, 2008, 39, 891-896.
78.   I. Sethmann, A. Putnis, O. Grassmann and P. Lobmann, *Am. Mineral.*, 2005, **90**, 1213-1217.
79.   J. Rieger, T. Frechen, G. Cox, W. Heckmann, C. Schmidt and J. Thieme, *Faraday discuss.*, 2007, **136**, 265-277.
80.   J. Termine and E. Eanes, *Calc. Tis Res.*, 1972, **10**, 171-197.
81.   J. R. Dorvee and A. Veis, *J. Struct. Biol.*, 2013, **183**, 278-303.
82.   J. R. Clarkson, T. J. Price and C. J. Adams, *J. Chem. Soc. Faraday Trans.*, 1992, **88**, 243-249.
83.   Y. Politi, J. Mahamid, H. Goldberg, S. Weiner and L. Addadi, *CrystEngComm*, 2007, **9**, 1171-1177.
84.   J. Aizenberg, J. Hanson, T. F. Koetzle, S. Weiner and L. Addadi, *J. Am. Chem. Soc.,* 1997, **119**, 881-886.
85.   J. Baumgartner, A. Dey, P. H. H. Bomans, C. Le Coadou, P. Fratzl, N. A. J. M. Sommerdijk and D. Faivre, *Nat. Mater.*, 2013, **12**, 310-314.
86.   D. Gebauer, M. Kellermeier, J. D. Gale, L. Bergstrom and H. Colfen, *Chem. Soc. Rev.*, 2014, **43**, 2348-2371.
87.   A. F. Wallace, L. O. Hedges, A. Fernandez-Martinez, P. Raiteri, J. D. Gale, G. A. Waychunas, S. Whitelam, J. F. Banfield and J. J. De Yoreo, *Science*, 2013, **341**, 885-889.

88. D. S. Li, M. H. Nielsen, J. R. I. Lee, C. Frandsen, J. F. Banfield and J. J. De Yoreo, *Science*, 2012, **336**, 1014-1018.
89. R. J. Park and F. C. Meldrum, *Adv. Mater.*, 2002, **14**, 1167-1169.
90. R. Blakemore, *Science*, 1975, **190**, 377-379.
91. D. A. Bazylinski and R. B. Frankel, *Nat. Rev. Microbiol.*, 2004, **2**, 217-230.
92. Y. A. Gorby, T. J. Beveridge and R. P. Blakemore, *J. Bacteriol.*, 1988, **170**, 834-841.
93. A. Scheffel, M. Gruska, D. Faivre, A. Linaroudis, J. M. Plitzko and D. Schuler, *Nature*, 2006, **440**, 110-114.
94. J. Baumgartner, G. Morin, N. Menguy, T. P. Gonzalez, M. Widdrat, J. Cosmidis and D. Faivre, *Proc. Natl. Acad. Sci. U.S.A.*, 2013, **110**, 14883-14888.
95. R. Robinson, *J. Bone Joint Surg.*, 1952, **34A**, 389-434.
96. S. Weiner and P. A. Price, *Calcif. Tissue Int.*, 1986, **39**, 365-375.
97. P. Fratzl, N. Fratzl-Zelman, K. Klaushofer, G. Vogl and K. Koller, *Calcif. Tissue Int.*, 1991, **48**, 407-413.
98. N. J. Crane, V. Popescu, M. D. Morris, P. Steenhuis and M. A. Ignelzi, Jr., *Bone*, 2006, **39**, 434-442.
99. M. J. Olszta, X. G. Cheng, S. S. Jee, R. Kumar, Y. Y. Kim, M. J. Kaufman, E. P. Douglas and L. B. Gower, *Mat. Sci. Eng. R.*, 2007, **58**, 77-116.
100. R. Wang and S. Weiner, *Connect. Tissue Res.*, 1998, **39**, 269-279.

ToC entry:

A working hypothesis for the understanding of amorphous-to crystalline transformations in biogenic skeletal materials forming through transient amorphous precursor phases.